In situ measurement of snowmelt infiltration under various topsoil cap thicknesses on a reclaimed site

Andre F. Christensen[1], Hailong He[1], Miles F. Dyck[1,3], E. Lenore Turner[1], David S. Chanasyk[1], M. Anne Naeth[1], and Connie Nichol[2]

[1]Department of Renewable Resources, 751 General Service Building, University of Alberta, Edmonton, Alberta, Canada T6G 2H1; and [2]Agrium, Inc., 1751 River Rd, Fort Saskatchewan, Alberta, Canada T8L 4J1.

Christensen, A. F., He, H., Dyck, M. F., Turner, L., Chanasyk, D. S., Naeth, M. A. and Nichol, C. 2013. **In situ measurement of snowmelt infiltration under various topsoil cap thicknesses on a reclaimed site**. Can. J. Soil Sci. **93**: 497–510. Understanding the soil and climatic conditions affecting the partitioning of snowmelt to runoff and infiltration during spring snow ablation is a requisite for water resources management and environmental risk assessment in cold semi-arid regions. Soil freezing and thawing processes, snowmelt runoff or infiltration into seasonally frozen soils have been documented for natural, agricultural or forested systems but rarely studied in severely disturbed systems such as reclaimed lands. The objective of this study was to quantify the snowmelt infiltration/runoff on phosphogypsum (PG) tailings piles capped with varying thicknesses of topsoil (0.15, 0.3, and 0.46 m) at a phosphate fertilizer production facility in Alberta. There are currently no environmental regulations specifying topsoil capping thickness or characteristics for these types of tailings piles. Generally, the function of the topsoil cap is to facilitate plant growth and minimize the amount of drainage into the underlying PG. Experimental plots were established in 2006 to better understand the vegetation and water dynamics in this reconstructed soil. In 2011, time domain reflectometry (TDR) probes and temperature sensors were installed at various depths for continuous, simultaneous, and automated measurement of composite dielectric permittivity (ε_{eff}) and soil temperature, respectively. An on-site meteorological station was used to record routine weather data. Liquid water and ice content were calculated with TDR-measured effective permittivity (ε_{eff}) and a composite dielectric mixing model. Spatial and temporal change of total water content (ice and liquid) revealed that snowmelt infiltration into the topsoil cap increased with increasing topsoil depth and net soil water flux from the topsoil cap into the PG material was positive during the snowmelt period in the spring of 2011. Given the objective of the capping soil is to reduce drainage of water into the PG material it is recognized that a capping soil with a higher water-holding capacity could reduce the amount of meteoric water entering the tailings.

Key words: Seasonally frozen soils, ground thermal regime, water and heat dynamics, phosphogypsum tailing, Fort Saskatchewan, snowmelt infiltration

Christensen, A. F., He, H., Dyck, M. F., Turner, L., Chanasyk, D. S., Naeth, M. A. et Nichol, C. 2013. **Quantification in situ des infiltrations de l'eau de fonte sous diverses épaisseurs de sol dans un site restauré**. Can. J. Soil Sci. **93**: 497–510. Comprendre les conditions du sol et du climat qui influent sur le partage de l'eau entre le ruissellement et l'infiltration à la fonte des neiges printanière est indispensable à la gestion des ressources hydriques et à l'évaluation des risques environnementaux dans les régions froides semi-arides. Les mécanismes du gel et du dégel du sol ainsi que le ruissellement des eaux de fonte ou leur infiltration dans le sol gelé de façon saisonnière sont bien documentés pour les systèmes naturels, agricoles et forestiers, mais on les a rarement étudiés dans les systèmes très perturbés comme les terres restaurées. L'étude que voici devait quantifier l'infiltration/le ruissellement de l'eau de fonte dans les tas de résidus de phosphogypse surmontés d'une couche variable de sol de surface (capuchon de 0,15, 0,3 et 0,46 m d'épaisseur), à une usine de fabrication d'engrais phosphatés de l'Alberta. À l'heure actuelle, aucun règlement sur l'environnement ne régit l'épaisseur du capuchon de sol ni les caractéristiques des tas de résidus de cette nature. En général, le capuchon de sol a pour but de faciliter la croissance des plantes et de minimiser le drainage vers la couche de phosphogypse sous-jacente. En 2006, on a aménagé des parcelles expérimentales pour mieux comprendre la dynamique de la végétation et de l'eau sur un sol ainsi reconstitué. Cinq ans plus tard, on a installé des réflectomètres temporels et des thermomètres à diverses profondeurs afin de mesurer de façon continue, simultanée et automatique la permittivité diélectrique des matériaux composites (ε_{eff}) et la température du sol, respectivement. Une station météorologique a été installée sur les lieux pour enregistrer les conditions climatiques. La quantité d'eau à l'état liquide et de glace a été calculée à partir de la permittivité ε_{eff} mesurée avec le réflectomètre et d'un modèle de mélange des fluides servant à déterminer les caractéristiques diélectriques des composites. La variation de la concentration totale d'eau (états liquide et solide) dans l'espace et le temps indique que l'infiltration de l'eau de fonte dans le capuchon de sol augmente avec l'épaisseur de la couche superficielle et que le flux net d'eau venant de

[3]Corresponding author (e-mail: miles.dyck@ualberta.ca).

Abbreviations: PG, phosphogypsum; **TDR**, time domain reflectometry

la surface et atteignant le phosphogypse avait été positif durant la fonte, au printemps 2011. Puisque le capuchon de sol a pour but de réduire le drainage de l'eau dans le phosphogypse, on convient qu'une couche retenant mieux l'eau pourrait réduire la quantité d'eau entraînant la météorisation qui pénètre dans la strate de résidus.

Mots clés: Sols gelés saisonnièrement, régime thermique du sol, dynamique de l'eau et de la chaleur, résidus de phosphogypse, Fort Saskatchewan, infiltration de l'eau de fonte

Snowmelt in cold, semi-arid areas may contribute to the recharge of soil water reservoirs and groundwater because of low evapotranspirational demand during spring snow ablation. Snowmelt, however, may become runoff if soil infiltration capacity is inhibited by ice lenses, ice-filled pores or a basal ice layer built up on the soil surface at the base of the snowpack (Cary et al. 1978; Kane 1980; Miller 1980). Snowmelt runoff can lead to an increased probability of erosion of fertile surface soils, migration of pesticides and other agricultural chemicals, and the potential for spring flooding (Janowicz et al. 2002; Hall et al. 2012). Partitioning of the snowmelt into soil water and runoff has important implications for water resource management strategies and the development of mitigation strategies to reduce environmental risks associated with dissolved or suspended contaminants.

Prediction of infiltration into seasonally frozen soils is much more complicated than that of infiltration into unfrozen soils since (1) water flow is strongly coupled with heat transport, hence both hydraulic and thermal properties of the soil affect the spatial and temporal variability of the processes; (2) phase changes between ice and infiltration water may occur; and (3) hydraulic properties are considerably influenced by the amount of ice and its spatial and temporal distribution. The infiltration capacity of partially frozen soils is governed by many factors such as soil-atmosphere energy exchange, soil thermal regime, quantity and rate of snow water release from the snowpack, heat content of the infiltrating water, thermal and hydraulic properties of the soil, soil structure, total soil water content prior to ground freezing or ice content at the time of snow melt, the number of freeze–thaw cycles that change total water and ice content during the winter time, and their complex interactions (Kane 1980; Stein and Kane 1983a; Granger et al. 1984).

Methods developed for unfrozen soils are commonly applied to frozen soils for measurement of infiltration rate into frozen soils. These methods include time domain reflectometry (TDR) (Stein and Kane 1983a; Iwata et al. 2008), double/single-ring infiltrometers (Kane and Stein 1983), neutron scattering (Granger et al. 1984), lysimeter (Kane 1978; Stähli and Lundin 1999), and dye tracing methods (Stähli et al. 2004). Total and liquid soil water content, soil temperature, matric potential, snow pack characteristics (i.e., snow depth and snow water equivalent), depth to groundwater table, and meteorological data (i.e., air temperature, precipitation, and albedo) are usually monitored concurrently to quantify snowmelt infiltration. Empirical expressions consisting of snow water equivalent and soil water content at melt time (Granger et al. 1984; Zhao and Gray 1997) and numerical models (Gray and Granger 1985; Stadler et al. 1997; Stähli and Lundin 1999; Gray et al. 2001; Zhao et al. 2002) have been developed to predict snow infiltration into frozen soils.

Of these above-mentioned methods, TDR can be easily multiplexed and automated making it widely used for both field and laboratory measurement of soil water content (Spaans and Baker 1995). The TDR technique is based on the measurement of the travel time of an electromagnetic wave pulse generated by a TDR cable tester through a wave guide (also called probe) inserted into a porous medium such as soil, unfrozen or frozen. The travel time of the wave through the probe is a function of the effective dielectric permittivity of soil, ε_{eff}, which in turn, is a function of permittivity of the individual constituents in the soil (air, water, solids and ice), their volumetric fractions, and geometric arrangements. Recent research (He and Dyck 2013) showed composite dielectric mixing models can be used to estimate unfrozen water content and ice content in frozen soils. The ability to monitor unfrozen water and ice content in the field may contribute to improving our understanding of snowmelt infiltration into partially frozen soils.

Extensive investigations of snowmelt infiltration behavior of frozen agricultural land (Zhao et al. 2002; Iwata et al. 2008), forested land (Stein and Kane 1983b; Stadler et al. 1997), prairie (Granger et al. 1984; Gray and Granger 1985), or alpine soil in the field as well as in cold chambers (Stadler et al. 2000) have been reported. No study was found by the authors for markedly disturbed systems such as reclaimed sites. Therefore the purpose of this research is to investigate snowmelt infiltration on reclaimed systems, and specifically, in a topsoil cap overlying phosphogypsum (PG) tailings.

Phosphogypsum is a by-product of the production of phosphoric acid, a necessary component in the production of phosphate fertilizers. The production of phosphoric acid involves the reaction of sulfuric acid and phosphate rock. The resulting solution is a combination of gypsum ($CaSO_4$), hydrogen fluoride and phosphoric acid (Rutherford et al. 1994). Once the PG material has been filtered from the solution, it is mixed with water to form a slurry which can be pumped into settling ponds (wet stacking). These settling ponds rise as the PG settles out of suspension, forming large stacks, referred to as PG stacks (Wissa 2002). The stacks can grow to

immense scales depending on the engineered capacity and can occupy vast amounts of land.

There may be numerous impurities in the phosphate source material including radium, uranium, arsenic, barium, cadmium, chromium, lead, mercury, selenium and phytotoxic fluoride (Rutherford et al. 1995). These trace elements may accumulate in the PG by-product and in the water held within its pore space. Studies have demonstrated that concentration and mobility of most trace elements within the PG pore water decreases with time as the stack drains (Rutherford et al. 1995). However, the introduction of precipitation into the PG stack may facilitate the mobility of these trace elements as well as dissolve the PG material (SENES 1987). Therefore, the leading concerns regarding PG stacks include contamination of the environment by multi-integrated vectors such as PG leachate to groundwater, wind and water dispersion to surrounding land and radionuclide emissions from the stack (SENES 1987; Thorne 1990) and stack stability.

The main objective of this work was to investigate the temporal and spatial changes of soil ice (θ_i) and liquid water (θ_l) content under various snow depths and topsoil cap thicknesses to understand the influences of freeze–thaw cycles on snowmelt infiltration into the topsoil caps and subsequent drainage (if any) into the underlying PG over the course of the spring thaw period in 2011 and the following 2011 freezing period and part of the spring, 2012 thaw. The relationship between snowmelt infiltration, snow depth, topsoil cap thickness and the soil freezing characteristic will be discussed throughout the paper.

MATERIAL AND METHODS

Site Description
The study was conducted at the Agrium Nitrogen Operations facility, located in Fort Saskatchewan, Alberta, Canada (lat. 53°44′07″N, long. 113°11′28″W, 624 m above the sea level). The area is described as cold, semi-arid having a mean annual temperature of 2.9°C and a mean annual precipitation of 460 mm, with 355 mm in the form of rainfall mainly occurring between May and August and 105 mm as snow. The average temperature from December through February is −11.7°C and 15.8°C from June through August (Environment Canada 2011). The growing season typically starts mid- to late April as marked by a mean daily temperature of >1°C for a period of 5 consecutive days. The growing seasons for the area typically last through to early September, when the maximum duration of sunshine, calculated from latitude and Julian day, decreases below 13.5 h (Hayashi et al. 2010).

The field site is permanently located on top of a decommissioned PG stack that was operational for 8 yr before its closure in 1991. The PG stack is approximately 15 m in height and occupies a base area of 9.3 ha. Eighteen (50 m × 10 m) plots were constructed atop the

decommissioned PG stack in a complete randomized design during the fall of 2006 (Jackson 2009). The plots were arranged into three replicates each containing six topsoil capping depth treatments including 8, 15, 30, 46, and 91 cm, as well as a 0-cm control; however, for the purposes of this research only replicate 2 was used for sampling due to the logistical constraints that were imposed with respect to site instrumentation. The general topography on which the topsoil was placed was relatively flat with a slope of <1%. Each topsoil depth treatment was further subdivided into five subplots (10 m × 10 m) that contained five different plant species treatments including *Agropyron trachycaulum* (Link) Malte ex H.F. Lewis (slender wheatgrass), *Agrostis stolonifera* L. (redtop), *Deschampsia caespitosa* (L.) P. Beauv. (tufted hairgrass), *Festuca ovina* L. (sheep fescue) and a mixture of 54% redtop, 2% slender wheatgrass, 28% tufted hairgrass, 8% sheep fescue and 8% alsike clover (Jackson 2009).

Topsoil and PG Characterization
The substrate that was used as the capping soil was a sandy loam to loamy sand textured Black Cherozemic soil excavated from a nearby alfalfa field. The capping soil had an average bulk density of 1.5 g cm^{-3} and an average porosity of approximately 0.44 cm^3 cm^{-3}. The saturated hydraulic conductivity of the topsoil cap was 7.4×10^{-3} cm s$^{-1} \pm 7.9 \times 10^{-5}$ (Jackson et al. 2011). Water retention curves for the topsoil indicated that the air entry potential for the topsoil material was approximately −28 cm and that the residual water content at −15 000 cm was 0.11 cm^3 cm^{-3} (Fig. 1).

The PG material matrix is dominated by silt sized particles that have a diameter ranging from 0.25 to 0.045 mm (Rutherford et al. 1994). Bulk density and porosity
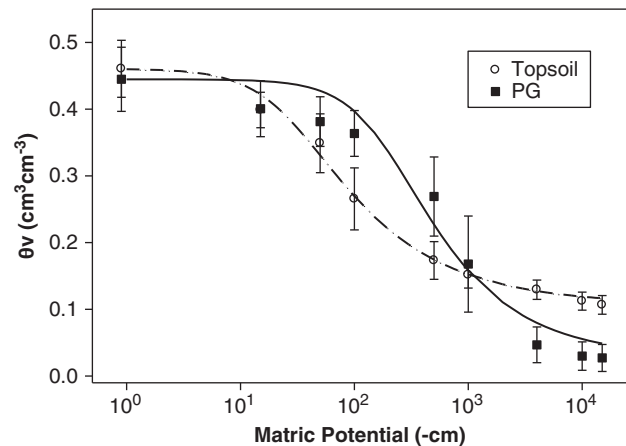
Fig. 1. van Genuchten (1980) model fitted to the moisture retention curves for the topsoil and PG material. van Genuchten parameters are $\alpha = 0.036$ cm^{-1}, $n = 1.57$, $\theta r = 0.11$ cm^3 cm^{-3}, $\theta s = 0.46$ cm^3 cm^{-3} for topsoil, and $\alpha = 0.0054$ cm^{-1}, $n = 1.67$, $\theta r = 0.027$ cm^3 cm^{-3}, $\theta s = 0.44$ cm^3 cm^{-3} for PG.

estimates for the PG material found on site averaged approximately 1.4 g cm^{-3} and 0.45 cm^3 cm^{-3}, respectively. The saturated hydraulic conductivity of PG material was 3.7×10^{-4} cm s$^{-1} \pm 6.6 \times 10^{-6}$ (Jackson et al. 2011). The water retention curve for the PG material indicated that the predicted air entry potential was approximately -186 cm and that the residual water content at $-15\,000$ cm was 0.03 cm^3 cm^{-3}; however, it is worth noting that the air entry potential is based on empirical parameters used in the van Genuchten model (Fig. 1). Some discrepancies regarding the fit of the van Genuchten model to the measured data are due in part to the finer-textured PG material and its narrow pore size distribution; therefore, the air entry potential would most likely be lower than the predicted value.

Experimental Design

The 15-, 30- and 46-cm treatments of replicate 2 were selected for soil water investigation based on the intended final reclamation depth, that would fall within the range of 15–46 cm as suggested by previous studies, and for the close proximity of each plot to one another that was necessary given the limitation of cable length for the TDR sensors (Jackson 2009; Hallin 2009). All experimental measurements were conducted within the *Agropyron trachycaulum* subplots of the three soil treatments in order to establish a controlled plant community that would be representative of the final reclamation goals.

Within each subplot, TDR probes were installed along with dielectric water potential sensors (MPS-1, Decagon Devices Inc., Pullman, WA) and soil temperature sensors (TMC50-HD, Onset Computer Corporation, Bourne, MA) (Table 1). The TDR probes and MPS-1s were horizontally installed at the soil/PG interface as well as 7.5 cm above and below the interface. Additional TDR probes were horizontally installed at 15-cm increments from the soil/PG interface as well as a single vertical probe installed into the topsoil cap

Table 1. Soil sensors and placement depth below soil surface

Soil treatment	Sensor	Depth
15 cm	TDR probe	7.5, 0^z, −7.5, −15, −30, −45 cm, and 15 cm vertical
	Temp. probe	7.5, 0^z, −7.5, −15, −30 and −45 cm
	MPS-1 probe	7.5, 0^z, and −7.5 cm
30 cm	TDR probe	15, 7.5, 0^z, −7.5, −15, −30, −45 cm, and 30 cm vertical
	Temp. probe	15, 7.5, 0^z, −7.5, −15, −30, and −45 cm
	MPS-1 probe	7.5, 0^z, and −7.5 cm
46 cm	TDR probe	30, 15, 7.5, 0^z, −7.5, −15, −30 cm, and 46 cm vertical
	Temp. probe	30, 15, 7.5, 0^z, −7.5, −15, and −30 cm
	MPS-1 probe	7.5, 0^z, and −7.5 cm

^{z}Soil/phosphogypsum interface.

equivalent to the soil treatment depth (15, 30 and 46 cm). The horizontal TDR probes were installed into a 60-cm × 50-cm trench that was dug to a depth of approximately 1 m using a backhoe in November of 2010. Once the TDR probes were installed the substrate material was repacked in the order in which it was removed in order to avoid mixing. The soil temperature probes were installed vertically into a narrow hole that was created within 50 cm of the TDR probes in April of 2011 due to winter conditions inhibiting earlier installation. Soil temperature sensors were installed at depths corresponding to the horizontal TDR probes for each subplot and subsequently routed to HOBO U12 external data loggers and logged on an hourly basis. The MPS-1 probes were routed to a CR 1000 data logger and monitored every 2 h [Campbell Scientific (Canada) Corp. 2007].

TDR Measurements

The TDR probes that were used during the experiment were constructed using two stainless steel rods, each with a diameter of 0.5 cm with 4-cm inter-rod spacing attached directly to a 10-m-long RG 58/U coaxial cable. Vertically installed TDR probes varied in length corresponding to topsoil treatment depth (15, 30 and 46 cm), while the horizontally installed TDR probes were a standardized length of 30 cm. The TDR probes that were installed were routed to 3 SDMX 50 multiplexers corresponding to the three subplots under investigation. The 3-SDMX 50 multiplexers were subsequently routed to a central multiplexer, which was connected directly to a TDR100 and CR 800 data logger [Campbell Scientific (Canada) Corp. 2007]. In order to reduce signal loss along the length of the cable RG 8/U coaxial cables were used to link the SDMX 50s to the central SDMX 50 multiplexer.

During spring melt and fall freeze up, electrical conductivity and the dielectric permittivity (ε_{eff}) were logged every 2 h, while the individual wave forms were logged every 6 h. During the mid-summer months the electrical conductivity and ε_{eff} were logged every 4 h and waveforms were logged every 12 h.

Meteorological Measurements

An on-site weather station was used to measure and record routine meteorological data on an hourly basis using a CR 10X data logger [Campbell Scientific (Canada) Corp. 2007]. Precipitation and solar radiation were measured using a TE525WS Texas Electronic 0.254 mm tipping bucket rain gauge and a Kipp & Zonen silicon pyranometer (SP-Lite), respectively. Wind speed and direction were measured using a 05103-10 RM Young wind monitor. Finally, air temperature and relative humidity were measured using a HMP45C Vaisala probe housed in a radiation shield [Campbell Scientific (Canada) Corp. 2007]. Snowfall data were measured at the Fort Saskatchewan

meteorological station, located 1.79 km south of the field site (Environment Canada 2012).

Snow Survey

Snow depth and density were measured on 2011 Feb. 26. The Fort Saskatchewan meteorological station, located 1.79 km away, was used after 2011 Feb. 26 to obtain further snow fall records. A snow survey was not conducted in 2012 due to the lack of cumulative snow pack; however, snowfall data were obtained from the nearby meteorological station in Fort Saskatchewan to estimate winter precipitation. For each 50 m × 10 m plot, 12 locations were selected for snow depth measurements (D, cm) using a standard ruler. Within each *Agropyron trachycaulum* subplot (10 m × 10 m) a single snow core was collected using a clear polyvinyl chloride tube (2.38-cm radius). For soil treatments with TDR probes installed the snow cores were collected within 50 cm of probe location. The snow cores were transferred to plastic sampling bags and weighed. The density of snow was used to compute snow water equivalent (mm) measurements for the plots under investigation.

Estimation of Unfrozen Water and Ice Content with TDR-measured ε_{eff}

Freezing of soils affects the dielectric permittivity similarly to the drying of unfrozen soils but the drying process in an unfrozen soil involves the replacement of water with air whereas the freezing process involves the displacement of water by ice. The dielectric permittivity of ice is about 3 times greater than air (3.2 compared with 1, respectively). Therefore, the ε_{eff} of a frozen soil will be greater than the ε_{eff} of an unfrozen soil with the same liquid water content if there is ice present. The amount of ice present is proportional to the water content prior to freezing and any water moving into the soil volume sampled by TDR probe.

He and Dyck (2013) showed that dielectric models could be used to calibrate TDR for the measurement of unfrozen water and ice content in frozen soils. Furthermore, He and Dyck (2013) presented evidence to show that the mixing models could be parameterized using unfrozen soil at a variety of water contents and then extended to frozen soils. However, the main limitation of this calibration method is that it only remains valid if the total water content (sum of ice and unfrozen water) within the measurement volume of the TDR probe remains constant while the soil is frozen. This condition is easy to satisfy in laboratory conditions, but may not always be satisfied in the field due to translocation and percolation of water within the soil profile. How this assumption affects the estimation of unfrozen water and ice content for the field measurements presented in this paper and their interpretation will be discussed in the results and discussion section.

To estimate the liquid water and ice content, the confocal ellispsoid model initially developed by Sihvola

and Lindell (1990) and further modified by He and Dyck (2013) was calibrated using unfrozen soil samples. Air-dry samples of the topsoil and PG were wetted with known quantities of deionized water to obtain various saturation levels, from air-dry to near saturation at increments of around 0.05 kg H_2O kg^{-1} soil and then equilibrated for at least 24 h at room temperature. The mixed soil samples at each of the prescribed moisture contents were then uniformly packed to a depth of 15 cm in a copper cylinder of 5.08-cm internal diameter in a range of bulk densities to test its influence on parameters of a specific soil. A TDR probe consisting of triple parallel stainless steel needles of 1.6 mm in diameter, 10 cm in length with 1-cm inter-rod spacing was inserted in the center of the cylinder, and connected to a TDR cable tester for measurement of ε_{eff}. Using this experimental data, the parameters for the mixing model were optimized using MathCad software such that the mean squared difference between TDR-measured ε_{eff} and the modeled ε_{eff} were minimized (Parametric Technology Corporation 2010).

Once a mixing model is parameterized, it can be used to estimate the unfrozen water content (θ_l) and the ice content (θ_i) given the measured ε_{eff}. However, the ε_{eff} in a frozen soil at a given temperature is dependent on the amount of ice present. The amount of ice present during a freezing process is proportional to the liquid water content prior to freezing and the temperature of the soil. To estimate the measured θ_l and θ_i, $\theta_l(\varepsilon_{eff})$ and $\theta_i(\varepsilon_{eff})$ calibration curves were simulated using the parameterized confocal ellipsoid model for the field-measured water content just prior to the onset of soil freezing (i.e., the initial water content prior to freezing) (Table 2). To simulate the calibration curves for each initial water content, ε_{eff} was calculated with the confocal ellipsoid model for a range of pairs of θ_l and θ_i, such that the total water content was always equal to the initial water content:

$$\theta_l + \theta_i \, \frac{\rho_i}{\rho_w} = \theta_{l,init} \tag{1}$$

where θ_l is the liquid, unfrozen water content (cm^3 cm^{-3}), θ_i is the ice content (cm^3 cm^{-3}), θ_{init} is the initial unfrozen water content prior to freezing, ρ_w is the density of water (assumed to be 1 g cm^{-3}) and ρ_i is the density of ice (assumed to be 0.9167 g cm^{-3}). The $\theta_l(\varepsilon_{eff})$ and $\theta_i(\varepsilon_{eff})$ for each are then constructed with linear interpolation between ε_{eff} and θ_l, and ε_{eff} and θ_i. The calibration curves are presented in Fig. 2.

The data presented in this paper were measured between 2011 Mar. 07 and 2012 Apr. 17. Soil temperature was not logged until 2011 Apr. 05 because cold conditions arrived earlier than expected in the previous fall and their installation was delayed. The TDR probes were installed prior to soil freezing in the fall of 2010, but data logging did not commence until March 2011. The initial water contents required for calculating
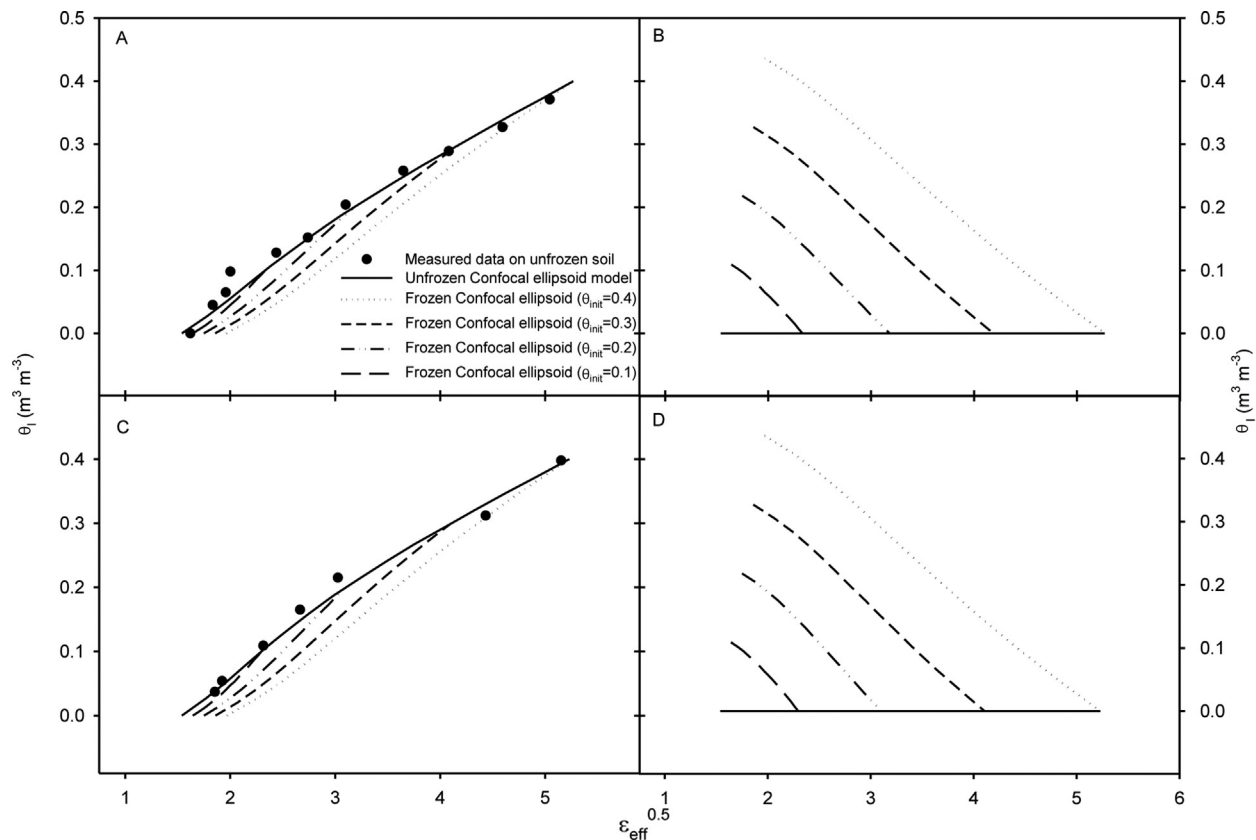
Fig. 2. TDR calibration curves for the estimation of liquid unfrozen water content (θ_l) and ice content (θ_i) for the topsoil cap (A & B) and the phosphogypsum (C & D).

unfrozen water and ice content in the frozen soil were measured gravimetrically on soil samples taken in the fall of 2010 (Turner 2013), and with the TDR data for the winter of 2011 and 2012. It is assumed that soil freezes at temperatures $\leq 0°C$ based on field tests that indicate that supercooling of soil water rarely occurs in the field (Golubev 1997). Ice contents, therefore, were only estimated when the soil temperature was $\leq 0°C$. (Miller 1980; Spaans 1996). Soil water content hereafter is referred to as liquid water content and the total water content is the sum of liquid water content and ice content. During the 2011 field season the snowmelt occurred between Mar. 29 and Apr. 15, while during the 2012 field season the snowmelt occurred between Mar. 12 and Apr. 05. The growing season for 2011 started on Apr. 23 and ended Sep. 01, the 2012 data analyzed in this paper ends prior to total soil thawing.

RESULTS AND DISCUSSION

Soil Freezing Processes in Different Thickness of Topsoil Treatments

For the 15-cm topsoil treatment, the time series of air temperature and precipitation, liquid water, ice, and soil temperature at six depths below the ground are presented in Fig. 3. Soil froze to a depth greater than 45 cm

(Fig. 3G) below the soil/PG interface in both winters and remained frozen well into the spring following snowmelt. The PG at 45 cm below soil/PG interface had completely thawed by 2011 May 17 and had not thawed as of 2012 Apr. 17 (Fig. 3G). An increased temperature lag was observed with increasing depth. During the 2011 snowmelt event, the topsoil reached near saturated conditions for a period of about 2 wk as a result of the reduced hydraulic conductivity of the underlying frozen PG material (Fig. 3D and E). The PG material directly below the interface began thawing on 2011 Apr. 21 marked by PG temperature that was $>0°C$ and an increase in liquid water content. The remaining frozen PG material at greater depths underwent similar phase changes for the following 26 d, after which point, the liquid water content stabilized at 0.35 cm^3 cm^{-3} for the remainder of the growing season. With respect to the topsoil, fluctuations in the water content above the soil/PG interface between May and November 2011 are due to periodic rainfall events followed by periods of evapotranspiration, potential drainage, and subsurface lateral flow. The summer rainfall events between mid-June and November 2011 negligibly affected the soil water content at depths greater than 7.5 cm below soil/PG interface, which
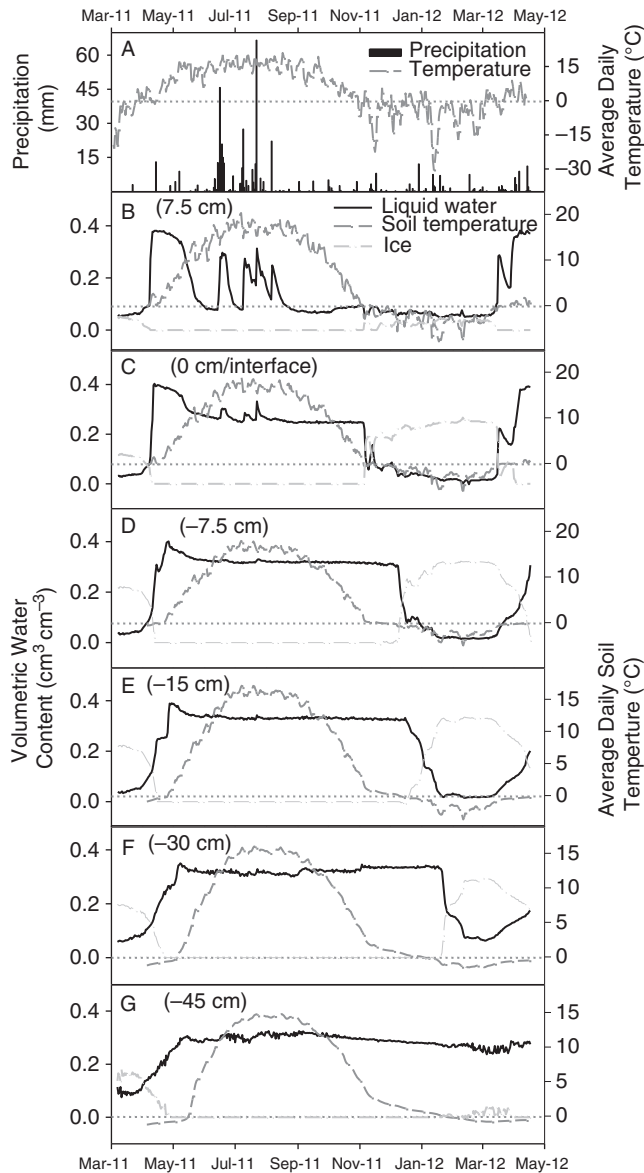
Fig. 3. Water and heat dynamics of 15 cm topsoil treatment during March 2011 to April 2012.

indicated that limited amounts of water percolated below the soil/PG interface and the water losses from the topsoil following precipitation events were from evapotranspiration or subsurface lateral flow. The hydraulic gradient across the soil/PG interface estimated with the matric potential sensors, however, suggests that there are discrete periods following precipitation events that could contribute to downward percolation which will be explored later in this paper.

Winter 2011–2012 was relatively warm compared with the previous 2010–2011 winter. The topsoil layer (Fig. 3B) was dry because of the low precipitation in the fall 2011 and as a result of limited winter precipitation

total soil water content remained relatively constant during the winter. Total soil water content at the soil/PG interface and below (Fig. 3C–G) was much higher at the onset of soil freezing (>0.3 cm^3 cm^{-3}) in the fall of 2011 and a significant drop in liquid water content was observed as soil froze. As the PG material froze, the estimated liquid water content decreased and the estimated ice content increased.

The soil water content at 7.5 cm above the soil/PG interface (Fig. 3B) increased concurrently with the snowmelt events and exceeded the initial water content indicating infiltration of snowmelt. Figure 3C shows a similar pattern to Fig. 3B in that percolation appeared to be restricted by the presence of ice in the underlying PG layer, which was a result of the high water content in the fall of 2010 (Fig. 3D). Although, a few thawing–freezing cycles occurred during the winter of 2012, only the refreezing event of 2012 Mar. 27 resulted in refreezing of infiltrating water.

Figures 4 and 5 illustrate the soil water content and temperature measurements for 30- and 46-cm topsoil cap treatments, respectively. Figure 3A, Fig. 4A and Fig. 5A are the meteorological conditions at the surface, but are repeated to show the correlation between surface boundary conditions and soil water dynamics.

Figures 4 and 5 are similar to Fig. 3 (15-cm treatment) in many respects. Steep increases in water content in the topsoil cap and PG during the snowmelt periods were observed. The date at which the snowmelt reached each depth increased with depth especially in the PG because the PG took longer to thaw. Liquid water content in the topsoil responded very rapidly to summer rainfall throughout the whole topsoil cap as indicated by the liquid water content response measured by the TDR probes at the soil/PG interface (Fig. 3C, Fig. 4D and Fig. 5E). The shallower the topsoil depth, the greater the magnitude of the response of the water content change to the rainfall events (i.e., Fig. 5B > Fig. 5C > Fig. 5D > Fig. 5E) but the PG water content did not change very much. The topsoil was relatively dry after August 2011 due to the small amounts of autumn rainfall. Total water content in the PG layers (Fig. 3D–G, Fig. 4E–G and Fig. 5F–G) remained relatively constant at approximately 0.35 cm^3 cm^{-3} during the periods after spring snowmelt event and before winter 2011. Despite the lack of snow in the winter of 2011–2012, snowmelt infiltration into the topsoil was very efficient because it was so dry from the previous fall. There is evidence of refreezing of snowmelt in the topsoil cap in March 2012, but this refreezing only resulted in a small amount of ice formation due to the initially dry soil conditions and as a result, infiltration was not inhibited. The observed water content at the interface of the three treatments was higher than the overlying topsoil cap, but lower than the underlying PG. The interface is generally the boundary between differing materials which may disrupt vertical water movement as discussed in Dyck and
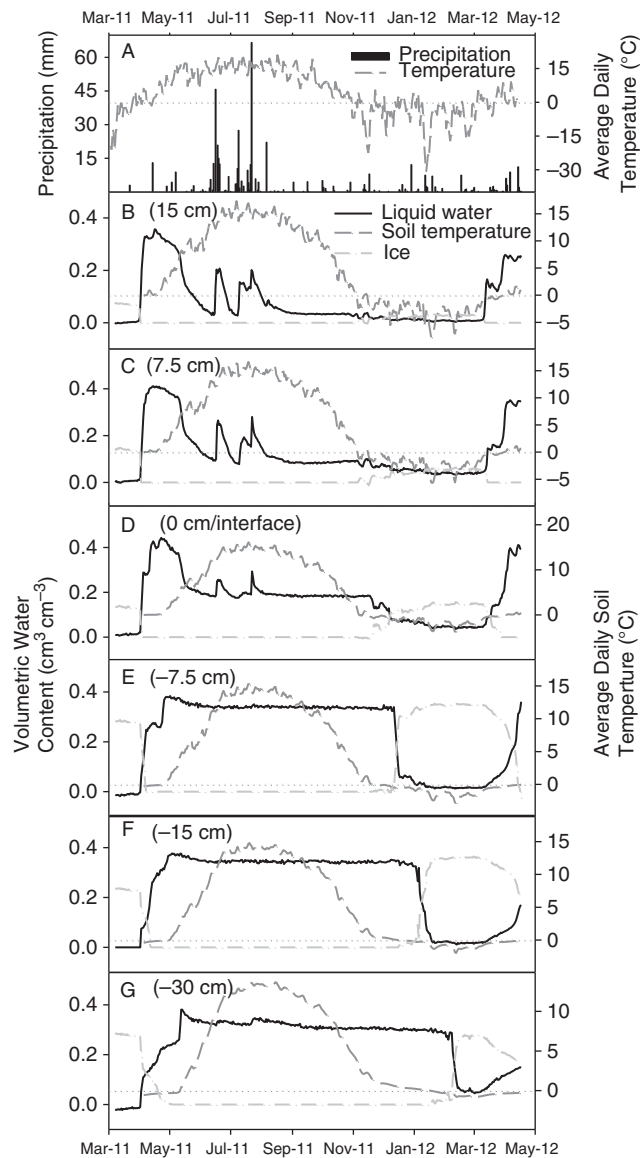
Fig. 4. Water and heat dynamics of 30 cm topsoil treatment during March 2011 to April 2012.

Fig. 5. Water and heat dynamics of 46 cm topsoil treatment during March 2011 to April 2012.

Kachanoski (2009). The water content at the interface of the 15-cm plot treatment (Fig. 3C) was consistently higher than that of the 30-cm treatment (Fig. 4D) and 46-cm treatment (Fig. 5D), which could be due in part to greater evapotranspirational demand from the 30- and 46-cm plots as evident by their slightly more robust plant growth during the growing season (not shown here). The variability among total soil water contents between the various plot interfaces may be explained by multiple factors including: (1) topographical variability of soil/PG gradients resulting in convergence or divergence of lateral flow; and (2) misrepresentative proportion of soil versus PG material within the sample volume of the horizontally installed TDR probes along the soil/

PG interface resulting in measurements more reflective of PG than of soil. Generally, the interface between the two layers is characterized by the very transient and variable moisture regime of the topsoil cap and very steady moisture regime in the PG.

The lack of fluctuation of water contents observed in the PG during the growing season is likely a result of the nature of the hydraulic properties between the soil and PG as well as the evapotranspirational demand of the active vegetation. However, increases in water content of the PG material at deeper depths were observed for the 30-cm plot following high magnitude precipitation events (Fig. 4G), which could be attributed to preferential flow paths. The decrease in water storage

within the topsoil cap could also be attributed to plant transpiration and potential subsurface lateral flow. Utilization of pore water from the PG material by the plants was minimal because of the lack of roots within the PG material. Field observations indicated that the majority of root material was located within the topsoil cap and concentrated on the soil/PG interface (L. Turner, 2013). The only time when the water content in the PG appeared to increase significantly was during soil thawing, suggesting deeper movement of snowmelt when the vegetation was still dormant.

Estimation of Cumulative Snowmelt Infiltration into Topsoil and Net Vertical Flux within PG

To better assess the performance of the various capping depths, the net water flux within the topsoil cap and the underlying PG material was quantified using the one-dimensional soil water continuity equation:

$$\frac{\partial \theta(z,t)}{\partial t} = \frac{\partial q(z,t)}{\partial z} \qquad (2)$$

Where θ is the total water content ($cm^3 \, cm^{-3}$), t is time (s), q is the soil water flux ($cm^3 \, cm^{-2} \, s^{-1}$) and z is depth (m). Integration of both sides of Eq. 2 between two depths (z1 and z2) results in:

$$\frac{\partial}{\partial t} \int_{z1}^{z2} \theta(z,t) dz = -\int_{z1}^{z2} \frac{\partial q(z,t)}{\partial z} dz \qquad (3a)$$

which may be expressed as:

$$\frac{\partial W_{z1,z2}(t)}{\partial t} = q(z1,t) - q(z2,t) \qquad (3b)$$

where $W_{z1,z2}(t)$ is the soil water storage between depths z1 and z2 as a function of time, and $q(z1,t)$ and $q(z2,t)$ are the net vertical soil water fluxes at depths z1 and z2, respectively. In other words, the change in soil water storage between depths z1 and z2 over a period of time is equal to the net soil water flux between those two depths over the same time period. For discrete time periods that are small enough such that $q(z1,t)$ and $q(z2,t)$ do not change significantly with time, Eq. 3b may be simplified to:

$$\Delta W_{z1,z2|\Delta t} = [q(z1) - q(z2)]\Delta t \qquad (4)$$

Which means the change in soil water storage between two depths measured at two discrete points in time is a result of the cumulative, net vertical flux occurring in the soil volume bounded by depths z1 and z2.

The cumulative, net vertical flux integrates fluxes affecting the change in total soil water storage between two depths such as infiltration, drainage, evapotranspiration and lateral flow over the time period in question. Positive changes in storage indicate that the cumulative flux coming into the soil volume (i.e., infiltration – evapotranspiration) bounded by z1 and z2 was greater than the net cumulative flux leaving that volume (i.e., percolation and other losses such as lateral flow), whereas decreases in soil water storage indicate the opposite. No change in soil water storage indicates a scenario where net water coming into the volume bounded by z1 and z2 was equal to the net water going out and those fluxes may or may not be zero.

Equation 4 was applied to two separate soil volumes, topsoil cap and PG, during periods of time during the snowmelt period and growing season. Estimates for the topsoil caps were calculated using the measurements from the vertically installed TDR probes and estimates for the PG material was calculated using the measurements from the horizontally installed probes at -7.5 and -15 cm for discrete time intervals during the snowmelt period of 2011. Setting z = 0 at the topsoil/PG interface with z increasing upward (Table 1) results in z1 = depth of topsoil, z2 = 0 cm for the topsoil cap, and z1 = 0 cm, z2 = -7.5 cm, z3 = -15 cm for the PG. The vertical probes spanned the entire depth of the topsoil cap. The vertical probes therefore, measured the average soil water content over the entire topsoil cap, which can then be used to estimate soil water storage by multiplying by the length of the TDR probe. For the horizontal probes in the PG, each TDR probe is assumed to represent the 3.75-cm of PG material above and below its location.

Time series of the vertical TDR probe measurements for the 2011 snowmelt period and growing season are shown in Fig. 6. Snowmelt began on 2011 Mar. 29 as marked on Fig. 6 when the average air temperature exceeded 0°C (solid grey vertical line in Fig. 6A). The start of infiltration was noted by the initial increase in volumetric water content (solid black vertical lines in Fig. 6B–D). Field observations noted that all snow had melted and infiltrated before 2011 Apr. 27.

During the spring snowmelt, the underlying PG material remained frozen limiting the amount of water able to drain from the topsoil cap. As a result of this condition the topsoil within the 15-cm plot approached near saturation during the early spring, while the 30- and 46-cm plots did not as a result of their increased storage capacity. Restrictions in flow between the soil and PG material can be attributed to the hydraulic nature of the underlying PG material, which has a saturated hydraulic conductivity that is an order of magnitude lower than that of the capping soil. However, the hydraulic conductivity is further lowered by the presence of ice-filled pore space within the PG material that had already thawed within the topsoil cap earlier in the spring. Water content in the topsoil caps began to decrease only when the underlying PG material had a temperature of > 0°C, indicating that the presence of ice was restricting percolation of water from the topsoil into the PG. On 2011 Apr. 23, the 15-cm plot started to lose water and 2011 Apr. 26 so did the 30- and 46-cm plots (dashed dark grey vertical lines in Fig. 6B–D). Before these dates the PG material directly underlying the capping soil had an average temperature < 0°C and can
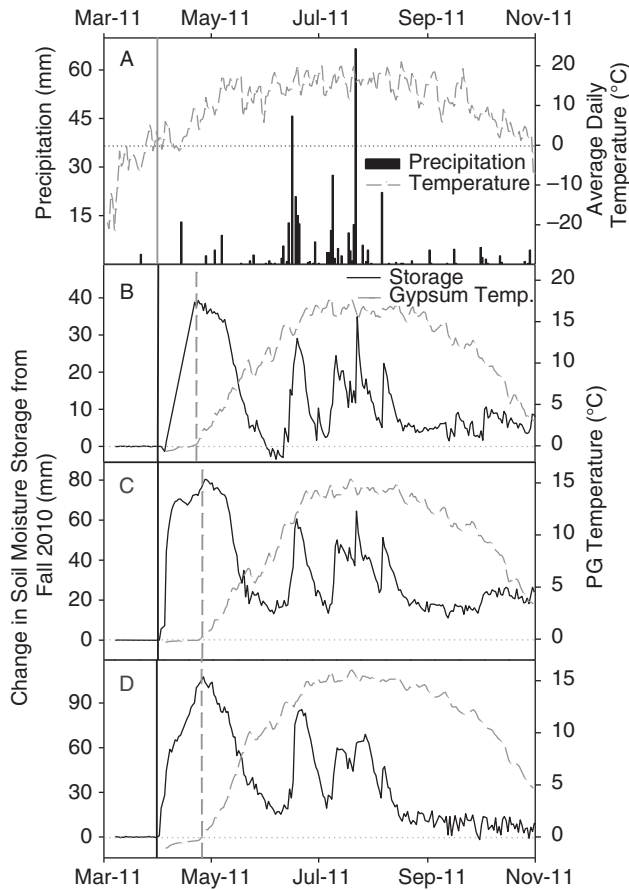
Fig. 6. Changes in storage within topsoil cap for the 15- (B), 30- (C) and 46-cm (D) capping soil treatments.

be assumed to have ice within the pore space restricting flow (Fig. 6B–D; Figs. 3–5).

Snowmelt infiltration into the topsoil cap was estimated between the beginning of snowmelt (2011 Mar. 29) and the beginning of the active growing season (2011 Apr. 23). Between these dates the potential evapotranspiration is negligible due to the limited photosynthetic ability of the plants during this part of the year where the average air temperature is <1°C. The amount of

infiltration into the topsoil cap as it pertains to available water from spring snowmelt (2011 Mar. 29 to Apr. 23) follows a general linear relationship with capping depth (Table 3). The estimates for infiltration for the 15-, 30- and 46-cm treatment are 38, 77 and 97 mm, respectively, indicating that an increase in soil capping depth results in an increase in infiltration of spring melt water into the capping soil. Conversely, this would suggest that the potential for runoff and/or subsurface lateral flow is highest in treatments where the topsoil is limited (i.e., ≤ 15 cm), due to the insufficient capacity of the topsoil to store the added water. Infiltration estimates for the 15- and 30-cm treatment would suggest that potential runoff and subsurface lateral flow could be occurring during snowmelt periods; however, the 46-cm treatment exhibits an excess amount of water within the topsoil cap than what was available from snowmelt and spring precipitation (Table 3). In this regard, more water has been observed to enter the 46-cm capping soil than is available from the environment. This phenomenon could be explained by localized variability in relief underlying the 46-cm plot that could contribute to the convergence of subsurface water flow as well as runoff water from the adjacent 15-cm plot. In general, the relationship between the amount of infiltration and capping soil thickness was linearly related, whereby the thicker the topsoil cap the greater the snowmelt infiltration capacity.

Estimates of net vertical flux can be measured from the amount of total water entering and leaving the PG as measured by the horizontally installed TDR probe directly below the soil/PG interface. Integrating the changes in total water content below the soil/PG interface with depth, from 2011 Apr. 23 to Sep. 01, gives an estimation of the net vertical flux below the interface during the entire growing season. This estimation is conservative with regards to the potential drainage because it does not take into account the potential percolation that could have occurred immediately following the snowmelt infiltration as represented by the hump in the water content distributions curves (Fig. 3D,

Table 2. Parameters of confocal ellipsoid models for estimating unfrozen water and ice content

	Parameters			
Soil type	Self-consistency	Aspect	RMSE[z]	Bulk density
Topsoil[y]	0.649	1	0.809	1.3
Gypsum[x]	0.537	1	0.918	1.2

[z]RMSE $= \frac{1}{N} \sum_{i=1}^{N} \varepsilon_i - \varepsilon_i$.
[y]Topsoil is Mundare loamy sand.
[x]Gypsum is phosphogypsum tailings.

Table 3. Estimates of cumulative spring infiltration into the topsoil cap and net storage and vertical flux within PG material over the 2011 growing season

Soil treatment	Available H$_2$O (SWE[z] + Precip.[y]) (mm)	Spring[x] cumulative infiltration – topsoil (mm)	Net cumulative vertical flux[vw] – PG (mm)
15 cm	88	38	20
30 cm	90	77	28
46 cm	82	97	32

[z]Snow water equivalent.
[y]Cumulative precipitation on site from 2011 Feb. 26 to Apr. 23.
[x]2011 Mar. 29 through to Apr. 23.
[w]15-cm-thick layer of phosphogypsum (PG) directly below soil/PG interface.
[v]2011 Apr. 23 to Sep. 01.

Fig. 4E, Fig. 5F). As a result of this simplification the net vertical flux estimates are reflective of the overall water balance within the PG material directly below the soil/PG interface, showcasing the net gains and/or losses during the entire 2011 growing season.

The cumulative, net vertical flux estimates (Eq. 4) over the entire growing season (2011 Apr. 23 to Sep. 01) for the PG layer directly below the interface were 20, 28 and 32 mm for the 15-, 30- and 46-cm treatments, respectively. The increase in the estimated cumulative, net vertical flux of the PG material with increasing topsoil depth is primarily due to the increased avail-ability of infiltrating spring snowmelt water that is present within each treatment. The more water that is available within the topsoil, from infiltration, the greater the potential will be for percolation and potential drainage. Although this result is counterintuitive with respect to conventional hypotheses regarding topsoil capping depth and drainage estimates, it can be ex-plained by the limited ability of the loamy sand material to retain water (Fig. 1) in combination with the in-creased amount of available water that is permitted to infiltrate into the topsoil. For example, the amount of water that infiltrated into the topsoil cap of the 15-cm treatment was 38 mm, which accounted for 43% of the available water during spring snowmelt, compared with that of the 30-cm treatment that allowed 86% of available water to infiltrate. The increased infiltration capacity of the thicker capping soils allows more water to enter into the system; however, the inability of the loamy sand material to retain the water allows for expedited redistribution of water within the reclaimed system resulting in increased estimates for net vertical flux with increased capping soil depth.

Direction of Net Vertical Flux

Changes in soil water storage, or net vertical flux, within the PG material, between the months of April and September 2011, are positive indicating that in general the amount of soil water entering into the PG from the topsoil cap is greater than the amount of soil water leaving the PG material; however, it can only be assumed that the water is percolating from the topsoil into the PG. To estimate the direction of flow total hydraulic head was quantified using the matric potential sensors installed at $+7.5$ and -7.5 cm from the soil/PG interface. The difference in total hydraulic head between $+7.5$ and -7.5 cm was used to obtain the hydraulic gradient across the interface.

During the snowmelt of 2011, the hydraulic gradients for the 15-, 30- and 46-cm treatment were all positive, indicating that the overall water flux was in the negative direction (downward) and that drainage/percolation was occurring. For the 15-, 30- and 46-cm treatments the gradients remained positive for 32, 47 and 39 d, respectively, from early April to mid-May, 2011 (Fig. 7). During this significant period of time soil water losses within the topsoil caps, following snowmelt infiltration,
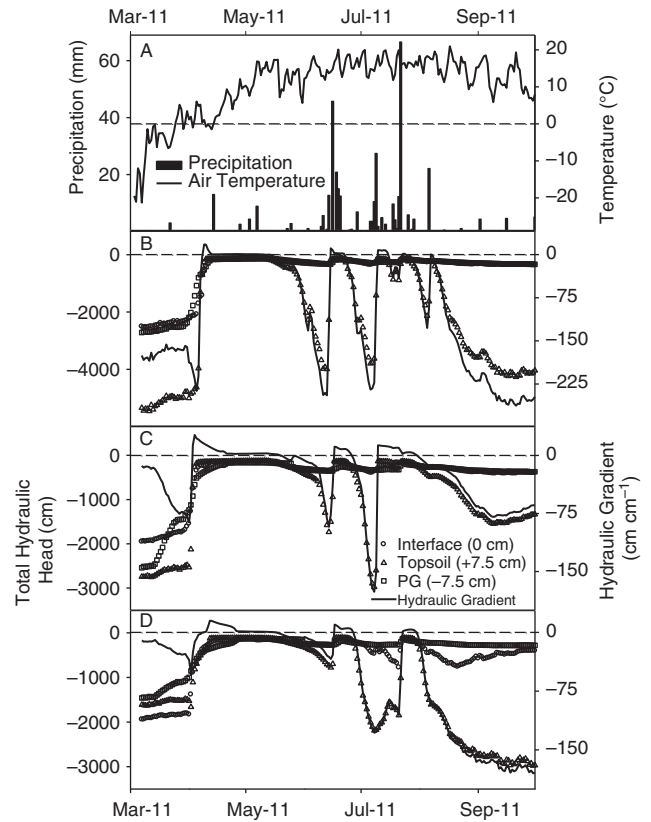
Fig. 7. Total hydraulic head and hydraulic gradient across soil/PG interface for the 15- (B), 30- (C) and 46-cm (D) capping soil treatments during March 2011 to November 2011.

is most likely primarily a function of drainage and can be minimally attributed to active evapotranspiration that was limited during the early spring. However, from mid-May through to September 2011 evapotrans-pirational demand increased, resulting in periods of negative hydraulic gradient across the interface, thus indicating upward water flux from the moist PG material to the drier loamy sand topsoil. This general summer trend was interrupted by several high magni-tude rainfall events on 2011 Jun. 16, Jul. 09 and Jul. 22, which produced 45, 27 and 66 mm of precipita-tion, respectively (Fig. 6A). During these rainfall events (>25 mm) positive hydraulic gradients were observed across the soil/PG interface for each of the topsoil treatments, indicating that drainage/percolation was occurring. The total amount of days from the start of snowmelt to the end of the growing season (2011 Mar. 29 to Sep. 01) that were observed to have drainage/percolation events present were 49, 78 and 57 for the 15-, 30- and 46-cm treatments, respectively. No trend appears to be present with regards to capping soil treatment and duration of drainage/percolation events; however, the 30-cm capping soil treatment was observed to have the longest periods of drainage/percolation,

accounting for 44% of the growing season, compared to that of the 15- and 46-cm treatments that have drainage/percolation estimates that account for 28 and 33% of the growing season (2011 Apr. 23 to Sep. 01).

Uncertainties in Soil Water, Infiltration and Net Flux Estimates

Sources of errors in the snowmelt infiltration estimates can be traced back to the distribution of water content measurements that were used to compute storage. As a result of increasing depth computation in deriving storage terms, the errors will linearly increase with increasing capping depth; however, variability between the various water content measurements during the steady state observations was very small (<0.01 cm^3 cm^{-3}). Other sources of error with regards to infiltration estimates include the possibility of steady state flow within the PG material during snowmelt periods. For example, the topsoil cap of the 15-cm treatment had a very high water content that remained stable during snowmelt infiltration, we assumed the lack of water movement was due to the limited ability of the frozen PG material to transmit the water; however, under steady state flow dynamics water content distribution within the topsoil cap would not change. The result of this assumption could have been an underestimation of the potential amount of available water infiltrating into the 15-cm plot; however, the evidence for limited flow dynamics below the soil/PG interface during the early spring snowmelt event indicated that water movement below the interface was limited as evident by the minimal increase in water content within the PG material prior to PG thaw. Furthermore, the hydraulic gradient across the soil/PG interface within the 15-cm plot remained negative until 2011 Apr. 09, indicating a positive flux direction; however, after 2011 Apr. 09 the interface temperature exceed 0°C and the hydraulic gradient reversed its direction, indicating drainage (Fig. 7). This does not entirely rule out the possibility of drainage during periods where there is no observable change in soil water storage in the topsoil cap, but it is likely very small if it does occur.

As mentioned above, TDR estimates of unfrozen water and ice content during periods when the soil is frozen are based on the assumption that the total water content within the sampling volume of the TDR probe does not change. Unfortunately, it is during times of snowmelt infiltration into frozen soils that this assumption is most likely to be violated. Because soil thawing and snowmelt infiltration both increase the liquid water content of the soil, there is some uncertainty associated with the unfrozen water and ice content estimates presented, especially in the more responsive topsoil cap. However, because of the very dry fall soil water conditions in the topsoil, these uncertainties are not expected to cause a misinterpretation of the processes occurring in the field. Furthermore, the estimates of net cumulative vertical flux are based on soil water measurements in unfrozen soil where the constant total water content assumption is no longer required.

CONCLUSION

TDR-estimated liquid water and ice contents in frozen soils were used to aid in the interpretation of hydrological processes in frozen soils at a reclaimed site. Results indicate that increases in capping soil thickness resulted in increases in infiltration of available snowmelt water into the capping soil and that lateral runoff estimates increased with decreasing capping depth. This result is primarily a response to the increase in the capacity of the deeper capping soils to infiltrate water; however, the limited ability of the loamy sand topsoil to retain water allows for the expedited redistribution of water within the reclaimed system. Therefore, greater capping soil depths appear to be associated with greater potential for percolation below the capping soil. Soil water balance estimates for the PG material directly underlying the treatment plots indicate that an increase in capping soil depth increased the net vertical flux within the first 15 cm of PG, which reflects the limited water retention characteristics of the topsoil. The estimated hydraulic gradient across the soil/PG interface indicates that during the early spring and severe precipitation events (>25 mm) drainage/percolation was occurring throughout all treatment depths; however, no clear trend was present in relation to treatment depth and duration of drainage/percolation events.

This research also confirms the importance of establishing very clear reclamation goals to aid in the selection of capping materials for mine tailings. At the minimum, a reclaimed tailing stack or pile should be able to support the establishment and maintenance of vegetation. It should limit exposure of environmental receptors to potential contaminants within the tailings. A soil with good infiltration and water-holding capacity should be able to aid in achieving these two goals. However, as shown in this paper, the thickness of the topsoil cap in combination with its infiltrability and water-holding capacity is a key consideration as well. Under the conditions reported in this paper a thicker topsoil cap resulted in greater water movement through the underlying PG tailings, which may or may not be desirable depending on the reclamation goals. Furthermore, moisture dynamics during freeze–thaw periods need to be taken into consideration when assessing reclamation goals and successful site reclamation.

Campbell Scientific (Canada) Corp. 2007. Products: sensors and supporting hardware [Online] Available: http://www.campbellsci.ca/Products_Sensors.html. [2011 Sep. 12].

Cary, J. W., Campbell, G. S. and Papendick, R. I. 1978. Is the soil frozen or not? An algorithm using weather records. Water Resour. Res. **4**: 1117–1122.

Dyck, M. F. and Kachanoski, R. G. 2009. Measurement of transient soil water flux across a soil horizon interface. Soil Sci. Soc. Am. J. **73**: 1604–1613.

Environment Canada. 2011. Canadian climate normal 1971–2000. [Online] Available: http://climate.weatheroffice.gc.ca/climate_normals/resultse.html?stnID=1886&lang=e&dCode=0&province=ALTA&provBut=&month1=0&month2=12. [2011 Mar. 15].

Environment Canada. 2012. National climate data and information archive. [Online] Available: http://www.climate.weatheroffice.gc.ca/advanceSearch/searchHistoricDataStations_e.html?searchType=stnName&timeframe=1&txtStationName=fort+saskatchewan&searchMethod=contains&optLimit=yearRange&StartYear=1840&EndYear=2012&Month=9&Day=21&Year=2012&selRowPerPage=25&cmdStnSubmit=Search. [2012 Mar. 20].

Golubev, V. V. 1997. Ice formation in freezing grounds. Pages 87–91 *in* S. Knutsson, ed. Ground freezing: frost action in soils. A. A. Balkema Publishers, Rotterdam, the Netherlands.

Granger, R. J., Gray, D. M. and Dyck, G. E. 1984. Snowmelt infiltration to frozen prairie soils. Can. J. Earth. Sci. **21**: 669–677.

Gray, D. M. and Granger, R. J. 1985. Snow management practices for increasing soil water reserves in frozen prairie soils. Proc. Watershed management in the eighties, Denver, CO.

Gray, D. M., Toth, B., Zhao, L. T., Pomeroy, J. W. and Granger, R. J. 2001. Estimating areal snowmelt infiltration into frozen soils. Hydrol. Process. **15**: 3095–3111.

Hall, D. K., Foster, J. L., DiGirolamo, N. E. and Riggs, G. A. 2012. Snow cover, snowmelt timing and stream power in the Wind River Range, Wyoming. Geomorphology **137**: 87–93.

Hallin, I. L. 2009. Evaluation of a substrate and vegetation cover system for reclaimed phosphogypsum stacks at Fort Saskatchewan, Alberta. M.Sc. thesis. University of Alberta, Edmonton, AB. 95 pp.

Hayashi, M., Jackson, J. F. and Xu, L. 2010. Application of versatile soil moisture budget model to estimate evaporation from prairie grassland. Can. Water Resour. J **35**: 187–208.

He, H., and Dyck, M. F. 2013. Application of multiphase dielectric mixing models for understanding the effective dielectric permittivity of frozen soils. Vadose Zone J. **12**: doi: 10.2136/vzj2012.0060.

Iwata, Y., Hayashi, M. and Hirota, T. 2008. Comparison of snowmelt infiltration under different soil-freezing conditions influenced by snow cover. Vadose Zone J. **7**: 79–86.

Jackson, E. M. 2009. Assessment of soil capping for phosphogypsum stack reclamation at Fort Saskatchewan, Alberta. M.Sc. thesis. University of Alberta, Edmonton, AB. 162 pp.

Jackson, E. M., Naeth, M. A., Chanasyk, D. S. and Nichol, C. K. 2011. Phosphogypsum capping depth affects revegeta-

tion and hydrology in western Canada. J. Environ. Qual. **40**: 1122–1129.

Janowicz, J. R., Gray, D. M. and Pomeroy, J. W. 2002. Characterization of snowmelt infiltration scaling parameters within a mountainous subarctic watershed. Proc. Eastern Snow Conference, Stowe, VT.

Kane, D. L. 1978. Snowmelt-frozen soil characteristics for a subarctic setting. Institute of Water Resources, University of Alaska, Anchorage, AK. 6 pp.

Kane, D. L. 1980. Snowmelt infiltration into seasonally frozen soils. Cold Reg. Sci. Technol. **3**: 153–161.

Kane, D. L. and Stein, J. 1983. Water movement into seasonally frozen soils. Water Resour. Res. **19**: 1547–1557.

Miller, R. D. 1980. Freezing phenomena in soils. Pages 254–299 *in* D. Hillel, ed. Applications of soil physics. Academic Press, New York, NY.

Parametric Technology Corporation. 2010. Mathcad Software Version 15.0 Student Edition. Parametric Technology Corporation, Needham, MA.

Rutherford, P. M., Dudas, M. J. and Arocena, J. M. 1995. Trace elements and fluoride in phosphogypsum leachates. Environ. Technol. **16**: 343–354.

Samek. 1994. Environmental impacts of phosphogypsum. Sci. Total Environ. **149**: 1–38.

SENES. 1987. An analysis of the major environmental and health concerns of phosphogypsum tailings in Canada and methods for their reduction. Prepared by: SENES Consultants Limited. Willowdale, ON. 560 pp.

Sihvola, A. H. and Lindell, I. V. 1990. Polarizability and effective permittivity of layered and continuously inhomogeneous dielectric ellipsoids. J. Electromagn. Waves Appl. **4**: 1–26.

Spaans, E. J. A. and Baker, J. M. 1995. Examining the use of time domain reflectometry for measuring liquid water content in frozen soil. Water Resour. Res. **31**: 2917–2925.

Stadler, D., Flühler, H. and Jansson, P. 1997. Modeling vertical and lateral water flow in frozen and sloped forest soil plots. Cold Reg. Sci. Technol. **26**: 181–194.

Stadler, D., Stahli, M., Aeby, P. and Fluhler, H. 2000. Dye tracing and image analysis for quantifying water infiltration into frozen soils. Soil Sci. Soc. Am. J. **64**: 505–516.

Stähli, M. and Lundin, L. C. 1999. Soil moisture redistribution and infiltration in frozen sandy soils. Water Resour. Res. **35**: 95–103.

Stähli, M., Bayard, D., Wydler, H. and Fluhler, H. 2004. Snowmelt infiltration into alpine soils visualized by dye tracer technique. Arct. Antarct. Alp. Res. **36**: 128–135.

Stein, J. and Kane, D. L. 1983a. Monitoring the unfrozen water content of soil and snow using time domain reflectometry. Water Resour. Res. **19**: 1573–1584.

Stein, J. and Kane, D. L. 1983b. Water movement into seasonally frozen soils. Water Resour. Res. **19**: 1547–1557.

Thorne, W. E. R. 1990. Reclamation of a phosphogypsum tailings pond: an examination of the relevant issues. MEDes thesis. University of Calgary, Calgary, AB. 330 pp.

Turner, E. L. 2013. Influence of soil cap depth and vegetation on reclamation of phosphogypsum stacks in Fort Saskatchewan, Alberta. M.Sc. thesis. University of Alberta, Edmonton, AB. 172 pp.

van Genuchten. M. Th. 1980. A closed-form equation for predicting the hydraulic conductivity of unsaturated soils. Soil Sci. Soc. Am. J. **44**: 892–898.

Wissa, A. E. Z. 2002. Phosphogypsum disposal and the environment. Pages 195–202 *in* Proc. of an international workshop on current environmental issues of fertilizer production. Prague, Czech Republic.

Zhao, L. and Gray, D. M. 1997. A parametric expression for estimating infiltration into frozen soils. Hydrol. Process. **11**: 1761–1775.

Zhao, L. T., Gray, D. M. and Toth, B. 2002. Influence of soil texture on snowmelt infiltration into frozen soils. Can. J. Soil Sci. **82**: 75–83.